JACS
JOURNAL OF THE AMERICAN CHEMICAL SOCIETY
Article
pubs.acs.org/JACS

In Situ Generation of Active Sites in Olefin Metathesis

Kazuhiko Amakawa, Sabine Wrabetz, Jutta Kröhnert, Genka Tzolova-Müller, Robert Schlögl, and Annette Trunschke*

Department of Inorganic Chemistry, Fritz-Haber-Institut der Max-Planck-Gesellschaft, Faradayweg 4-6, 14195 Berlin, Germany

Supporting Information

ABSTRACT: The depth of our understanding in catalysis is governed by the information we have about the number of active sites and their molecular structure. The nature of an active center on the surface of a working heterogeneous catalyst is, however, extremely difficult to identify and precise quantification of active species is generally missing. In metathesis of propene over dispersed molybdenum oxide supported on silica, only 1.5% of all Mo atoms in the catalyst are captured to form the active centers. Here we combine infrared spectroscopy in operando with microcalorimetry and reactivity studies using isotopic labeling to monitor catalyst formation. We show that the active Mo(VI)−alkylidene moieties are generated in situ by surface reaction of grafted molybdenum oxide precursor species with the substrate molecule itself gaining insight into the pathways limiting the number of active centers on the surface of a heterogeneous catalyst. The active site formation involves sequential steps requiring multiple catalyst functions: protonation of propene to surface Mo(VI)−isopropoxide species driven by surface Brønsted acid sites, subsequent oxidation of isopropoxide to acetone in the adsorbed state owing to the red-ox capability of molybdenum leaving naked Mo(IV) sites after desorption of acetone, and oxidative addition of another propene molecule yielding finally the active Mo(VI)−alkylidene species. This view is quite different from the one-step mechanism, which has been accepted in the community for three decades, however, fully consistent with the empirically recognized importance of acidity, reducibility, and strict dehydration of the catalyst. The knowledge acquired in the present work has been successfully implemented for catalyst improvement. Simple heat treatment after the initial propene adsorption doubled the catalytic activity by accelerating the oxidation and desorption-capturing steps, demonstrating the merit of knowledge-based strategies in heterogeneous catalysis. Molecular structure of active Mo(VI)−alkylidene sites derived from surface molybdena is discussed in the context of similarity to the highly active Schrock-type homogeneous catalysts.

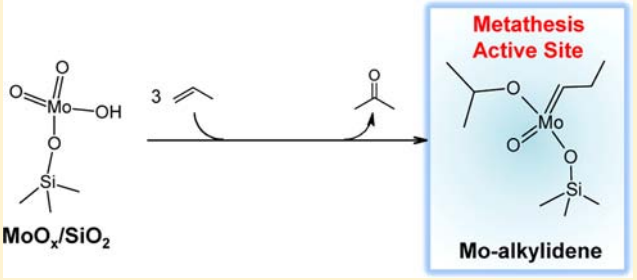

1. INTRODUCTION

Despite the vital branch of industrial production that involves heterogeneous catalysis, underlying research in the entire range of complexity from model studies over single-crystals to the investigation of applied catalyst formulations generally lacks in the most essential information: structure and number of active sites.[1] The termination of the solid surface that represents the catalytic interface is, even for model catalysts, enormously diverse[2] and changes dynamically under reaction conditions.[3,4] Hence, despite significant progress in the field of molecular surface science,[2−4] identification of catalytically relevant surface structures (i.e., active sites) among the existing variety of structures and counting of active sites remains extremely challenging, and the catalyst is still a "Holy Grail".[1] Heterogeneous olefin metathesis is an exceptional case where the general structural motif of active sites is established and thus quantification is accessible.[5] It is generally accepted that metal carbene species (M═CHR) catalyze the reaction according to the metallacyclobutane intermediate mechanism in analogy to homogeneous catalysis.[6] Irrespective of the specific metal carbene structure, quantification of active sites is possible applying postreaction metathesis using a probe olefin.[5,7,8]

Monolayer-type metal (e.g., Mo, W, and Re) oxides deposited on porous supports (e.g., silica, alumina, and silica−alumina) are important metathesis catalysts.[9−14] The number of active carbene species in these catalysts is at most 2% of the total metal content.[5,7,8] The low abundance is attributed to multiple geometric configurations, allowing only a minor fraction of surface metal oxide species to be transformed into the metal carbene upon contact with the olefin. Understanding the formation mechanism of the active centers and their in-depth structural description will provide the criteria for the relevant precursor structures disclosing access to more sustainability and improved economics via rational catalyst design.

The surface reaction between catalyst precursor and olefin is a demanding process, since the metal oxides need to accomplish carbene synthesis in one-pot and in situ. Several surface reactions via different intermediates have been proposed

Received: February 6, 2012
Published: June 15, 2012

   dx.doi.org/10.1021/ja3011989 | J. Am. Chem. Soc. 2012, 134, 11462−11473

(Scheme 1): (A) formation of a π-complex between the reacting alkene and a coordinatively unsaturated metal ion

Scheme 1. Proposed Mechanisms for Initial Carbene Formation upon Contact of the Catalyst with an Olefin[a]

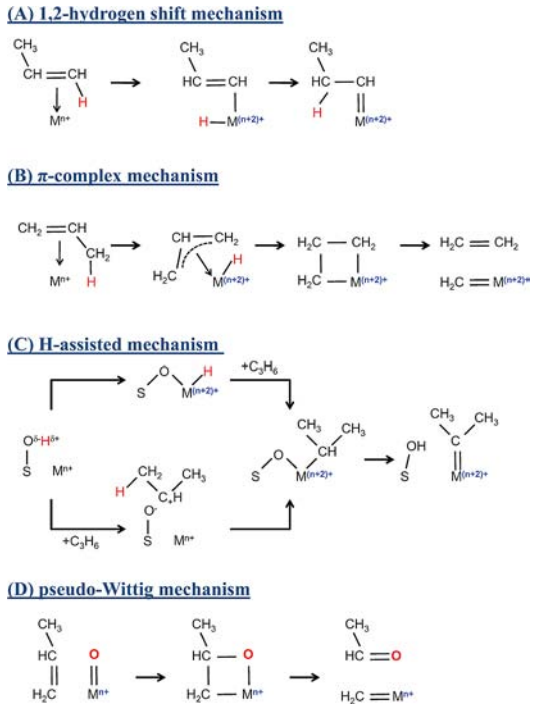

[a]M = active metal center for metathesis reaction, S = support element.

followed by a 1,2-hydrogen shift (1,2-hydrogen shift mechanism),[15,16] (B) formation of a π-complex followed the transformation of the π-allyl hydride intermediate into a metallacyclobutane (allyl mechanism),[17−19] (C) formation of a metal-oxo intermediate mediated by a surface Brønsted acid site and subsequent hydrogen shift (H-assisted mechanism),[20] and (D) formation of an oxametallacyclobutane and subsequent elimination of a carbonyl compound (pseudo-Wittig mechanism).[7,21−24]

All reaction pathways, except the pseudo-Wittig mechanism, involve an oxidative addition reaction, in which metal centers are required that can be oxidized by losing two electrons. Since catalyst pretreatment and regeneration of supported metal oxides are typically performed by oxidative treatment at elevated temperature,[9,25] the pseudo-Wittig mechanism would be the only applicable carbene formation route.

In this work, we describe the origin of active carbene species in propene metathesis over a well-defined model catalyst that contains dispersed molybdenum oxide species supported on meso-structured silica. We investigated propene adsorption using microcalorimetry and in situ IR spectroscopy to trace the genesis of active carbene sites. Our experimental findings deny the pseudo-Wittig mechanism, and provide a new picture, which is fully consistent with the empirical criteria for high-performing catalysts. The established mechanism allows sorting out possible molecular structures of surface oxide precursor species and resulting metal carbene configurations and resulted in the successful implementation of a new catalyst pretreatment procedure. The molecular structure of metal carbene species derived from surface molybdena is discussed in the context of similarities to highly active Schrock-type homogeneous catalysts.

2. EXPERIMENTAL SECTION

The experimental details are presented in the Supporting Information, SI. Below, the most important information is briefly summarized.

2.1. Preparation of MoO_x/SBA-15. Molybdenum oxide was dispersed on the surface of mesoporous silica SBA-15[26] applying an anion exchange procedure.[27] According to this, freshly prepared SBA-15 (specific surface area (S_{BET}) = 859 m^2 g^{-1}, internal sample ID 8233) was at first functionalized with propylammonium chloride using (3-aminopropyl)trimethoxysilane followed by treatment with hydrochloric acid. Then, anion exchange employing an aqueous solution of ammonium heptamolybdate was performed. After washing and filtration, the material was dried and calcined at 823 K in air to remove organic moieties as well as chlorine and to anchor molybdena species on silica, yielding MoO_x/SBA-15 with actual molybdenum loading of 9.7%, which corresponds to the surface molybdenum density of 1.1 Mo/nm^2 (S_{BET} = 556 m^2 g^{-1}, internal sample ID 8438). The nitrogen adsorption study (Table S1, Figure S1 of the SI) confirmed that the cylindrical mesopore structure of the SBA-15 was preserved after the molybdenum loading. Due to the decrease in the S_μ/S_{BET} ratio (Table S1 of the SI), preferential filling of the micropores with molybdenum oxides is suggested.

2.2. Physico-Chemical Characterization of MoO_x/SBA-15. Nitrogen adsorption was carried out at 77 K to determine specific surface area S_{BET}, micropore surface area S_μ, pore volume, and pore size distribution. X-ray fluorescence (XRF), powder X-ray diffraction (XRD), ultraviolet−visible (UV−vis) diffuse reflectance spectroscopy using SBA-15 as reference, Raman spectroscopy applying an excitation wavelength at 632.8 nm, and laser power of 1.5 mW at the sample position, and diffuse reflectance infrared Fourier transform (DRIFT) spectroscopy using KBr as reference were employed to characterize the catalyst and the support. Prior to Raman, DRIFT, and UV−vis spectroscopy, the samples were pretreated at 823 K (heating rate 10 K·min^{-1}) for 0.5 h in a dry 20% O_2 in Ar flow. To probe acidity, ammonia adsorption FTIR was performed in transmission mode using self-supporting wafers. Ammonia was adsorbed at 353 K after pretreatment of the samples at 823 K in dry oxygen.

2.3. Propene Metathesis. Catalytic activity in metathesis of propene to ethene and 2-butenes was measured using a fixed-bed tubular flow reactor at atmospheric pressure. The catalyst bed was pretreated at 823 K for 0.5 h in a flow of a thoroughly dried gas mixture of 20% O_2 in Ar, cooled to 323 K in the same gas flow, and then flushed with a flow of Ar before reaction. Dried and deoxygenated neat propene was fed to the catalyst bed at 323 K at atmospheric pressure. Inlet and outlet gases were analyzed by online gas chromatography. The selectivity to the metathesis products (ethene, *cis*- and *trans*-butene) was higher than 99.5%, while trace amounts of 1-butene and higher hydrocarbons were detected. The activity is presented as formation rate of the metathesis products (i.e., sum of ethene, *cis*- and *trans*-butene) normalized to the mass of the catalyst. Regeneration of the catalyst was performed using the same procedure as the initial activation.

2.4. Postreaction Ethene-d_4 Metathesis for Active Site Counting. A modified version of the dynamic active site counting technique originally developed by Handzlik[5] was employed, wherein ethene-d_4 (CD_2=CD_2) was used instead of nonlabeled ethene as the probe olefin to titrate metal carbene centers after the catalysis. According to the Chauvin mechanism[6] (Scheme 2), equal amounts of molybdenum methylidene (Mo=CH_2) and molybdenum ethylidene (Mo=CH−CH_3) species are present under steady state conditions of propene metathesis on the catalyst surface. The active site counting consists of the quantification of molybdenum-ethylidene (Mo=CH−CH_3) species by titration with ethene-d_4 (CD_2=CD_2), which results in liberation of propene-1,1-d_2 (CD_2=CH−CH_3) via metathesis reaction according to eq 1 and Scheme 2.

$$CD_2{=}CD_2 + Mo{=}CH{-}CH_3 \rightarrow CD_2{=}CH{-}CH_3 + Mo{=}CD_2 \quad (1)$$

dx.doi.org/10.1021/ja3011989 | J. Am. Chem. Soc. 2012, 134, 11462−11473

Scheme 2. Reaction Mechanism of Propene Metathesis According to Chauvin[1a]

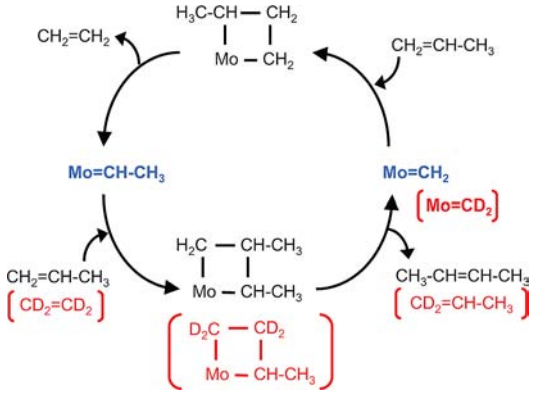

[a]The titration reaction of Mo−ethylidene with ethene-d_4 is described in red color.

Subsequent to the metathesis reaction, the reactor was flushed with flowing Ar, then the feed gas was switched to 1% C_2D_4 in Ar at 323 K. The formation of propene-1,1-d_2 was monitored and quantified with a quadrupole mass spectrometer (QMS200, Balzer) using the signal of m/z = 43. The active site density corresponds to the 2-fold amount of liberated propene-1,1-d_2 normalized to the weight of the catalyst.

2.5. Microcalorimetry and in Situ IR Spectroscopy of Propene Adsorption. Microcalorimetry was performed using a MS70 Calvet Calorimeter (SETRAM). The calorimeter was combined with a custom-designed high vacuum and gas dosing apparatus equipped with a volumetric system, which allows measurements of adsorption isotherms. The IR experiments were carried out in transmission mode using a Perkin-Elmer 100 FTIR spectrometer equipped with an in situ cell. In both methods, propene was admitted at 323 K after pretreatment of the catalyst in 20 kPa of oxygen at 823 K for 0.5 h and subsequent evacuation at 323 K. Adsorption of C_2D_4 after propene adsorption as well as adsorption of isopropanol and acetone were also conducted in the IR study.

3. RESULTS

3.1. Physico-Chemical Characterization of MoO_x/SBA-15. After the oxidative pretreatment, highly dispersed molybdenum oxide species with molybdenum in the highest oxidation state exist on the catalyst surface. The presence of bulk-like MoO_3 and $H_4SiMo_{12}O_{40}$ impurities is excluded not only due to the absence of any related reflection peak in the XRD patterns (not shown), but, in particular, due to the lack in bands at 816 cm^{-1} for MoO_3, and 909 cm^{-1} for $H_4SiMo_{12}O_4$[28] in the Raman spectrum (Figure S2 of the SI). The Raman bands near 990 and 970 cm^{-1} due to molybdenum−oxygen stretching vibrations (νMo═O) (Figure S2 of the SI) as well as the absorption bands in the UV−vis spectrum near 225 and 270 nm (ligand to metal charge transfer from O^{2-} to Mo^{6+}) (Figure S3 of the SI) are typical fingerprints indicating highly dispersed molybdenum oxide surface species in the dehydrated state.[28−31] The absence of absorption due to d−d transitions of molybdenum ions (>500 nm)[32] is evidence that molybdenum is exclusively present as Mo(VI).

The DRIFT spectrum (Figure 1A) of MoO_x/SBA-15 shows significantly weaker intensity of the band due to isolated Si−OH (silanol) groups[33] at 3745 cm^{-1} than bare SBA-15, indicating that loading of molybdenum involves consumption of surface silanol groups to yield anchored surface molybdate species. Moreover, the DRIFT spectrum of MoO_x/SBA-15 features a broad OH stretching mode at 3620 cm^{-1}, which

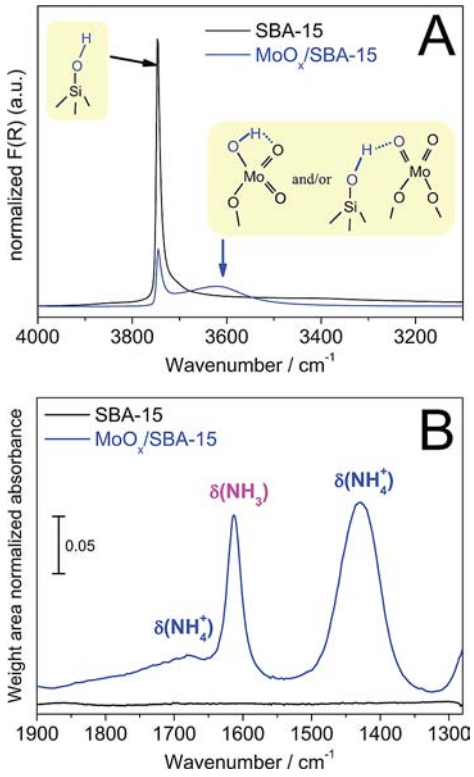

Figure 1. IR spectra of MoO_x/SBA-15 and SBA-15; (A): DRIFT spectra measured at room temperature after pretreatment in 20% O_2 at 823 K for 0.5 h. (B): Transmission IR spectra recorded after adsorption of ammonia at p = 10 hPa and subsequent evacuation at 353 K. The catalyst was pretreated in 20 kPa of O_2 at 823 K for 0.5 h. The spectrum before ammonia dosing was used as background.

clearly indicates the occurrence of hydrogen-bonded OH groups when molybdenum is loaded onto the silica SBA-15 surface. The latter band is attributed to a superposition of O−H stretching vibrations in molybdenol (Mo−OH) groups involved in hydrogen bonding to neighboring oxygen atoms, e.g., in O═Mo−OH moieties or silanol groups that undergo hydrogen interaction with oxygen atoms of molybdena species in the vicinity.

The adsorption of ammonia revealed the presence of both Brønsted and Lewis acid sites. Whereas almost no ammonia adsorbs on SBA-15 (black line in Figure 1B), the IR spectrum of MoO_x/SBA-15 after ammonia adsorption (blue line in Figure 1B) shows the presence of ammonium ions formed by reaction of NH_3 with Brønsted acid sites (1678 cm^{-1} ($\delta_{sym}NH_4$) and 1431 cm^{-1} ($\delta_{as}NH_4^+$)) and molecular ammonia coordinated at Lewis acid sites (1613 cm^{-1} ($\delta_{as}NH_3$)).[33] The detection of Brønsted acid sites indicates either the presence of molybdenol (Mo−OH) groups or the formation of acid Si−OH groups by interaction of terminal silanol groups with surface molybdenum oxide species. The broad OH stretching mode at 3620 cm^{-1} detected in MoO_x/SBA-15 (Figure 1A) may contain contributions from either of them. Lewis acid sites are considered as coordinatively unsaturated Mo(VI) centers. Irrespective of the specific assignment, ammonia adsorption clearly indicates the generation of acid sites by introduction of molybdenum oxide species into the pores of SBA-15.

In summary, the MoO_x/SBA-15 model catalyst is characterized by extensive coverage of the silica surface with highly dispersed MoO_x species containing Mo in its highest oxidation

dx.doi.org/10.1021/ja3011989 | J. Am. Chem. Soc. 2012, 134, 11462−11473

state, and comprising Mo oxo (Mo═O) moieties. The presence of Brønsted acid sites and coordinatively unsaturated Mo(VI) species (Lewis acid sites) is evidenced by ammonia adsorption IR.

3.2. Propene Metathesis and Postreaction Active Site Counting. Figure 2 shows the propene metathesis activity of

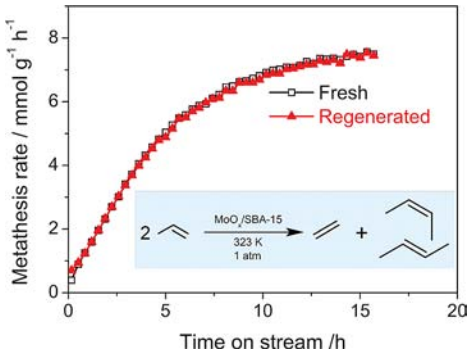

Figure 2. Propene metathesis activity of MoO_x/SBA-15 at 323 K and a contact time of 0.75 s g mL^{-1}. The catalyst was activated in a 20% O_2 flow at 823 K for 0.5 h. Regeneration was performed applying the same procedure as the initial activation (823 K in 20% O_2 for 0.5 h).

MoO_x/SBA-15 at 323 K as a function of time on stream. The metathesis activity gradually develops with time on stream, reaching 7.5 mmol g^{-1} h^{-1} (corresponding to an apparent TOF of 2.06 $mmol_{propene}$ mol_{Mo}^{-1} s^{-1}) after 15 h. Metathesis activity and apparent TOF are rather low compared to the recent most successful silica−alumina supported molybdena catalysts reported by Debecker et al.[11,12] The gradual evolution of the activity suggests slow generation and continuous accumulation of active molybdenum carbene centers.[34] The catalyst is regenerable with an excellent reproducibility in the reactivity (Figure 2).

Table 1 summarizes the data on the metathesis activity and the postreaction active site counting as well as the derived

Table 1. Summary of Propene Metathesis Activity and Post-Reaction Active Site Counting over MoO_x/SBA-15

catalyst	activity[a] (mmol g^{-1} h^{-1})	active sites[b] (μmol g^{-1})	active site fraction[c] (atom%)	TOF[d] (s^{-1})
fresh	7.50	15.0	1.5	0.14
regenerated	7.44	14.0	1.4	0.15

[a]Propene metathesis activity measured immediately before the postreaction active site counting procedure (TOS = 15 h) for MoO_x/SBA-15 (see also Figure 2); Metathesis reaction condition: T = 323 K, p = 0.1 MPa, contact time = 0.75 s ml g^{-1}, pretreatment or regeneration at T = 823 K for 0.5 h under 20% O_2−Ar flow. [b]The 2-fold amount of evolved propene-d_2 upon ethene-d_4 dosing after the propene metathesis. [c]Active site density divided by Mo loading. [d]Metathesis activity divided by active site density.

active site fraction and turn over frequencies. The active site density corresponds to about 1.5% of total molybdenum atoms in the catalyst. The value is similar to reported data on MoO_x/Al_2O_3[5] and ReO_x/Al_2O_3.[7,8]

3.3. Microcalorimetry of Propene Adsorption at the Reaction Temperature. To gain insight into the process of carbene site formation, we studied propene adsorption by microcalorimetry at the reaction temperature. The metathesis reaction does not disturb the calorimetric measurement, because (1) the heat of reaction is very small (ΔH_{323K} = 1.2 kJ $mol_{propene}^{-1}$) and, consequently, thermal contributions from the catalytic reaction can practically be neglected in the measurement of the heat of adsorption, and (2) the total number of molecules remains constant through the reaction, which allows volumetric determination of the amount of adsorbed propene molecules because the total pressure is not falsified due to the reaction. This situation opens up the opportunity to trace thermal events, which are presumably relevant to the genesis of activity.

Figure 3 A,B reports the differential heat of propene adsorption on MoO_x/SBA-15 (A) and SBA-15 (B) as a function of propene coverage. While the differential heat measured on SBA-15 is slightly higher than the heat of propene condensation and remains constant at 23 ± 1 kJ mol^{-1} with increasing coverage (Figure 3B), the MoO_x/SBA-15 catalyst shows significantly higher heats of adsorption up to certain levels of coverage (Figures 3A). The catalyst MoO_x/SBA-15 (Figure 3A) is characterized by a plateau up to 16 μmol g^{-1}, which corresponds to 1.6% of total molybdenum atoms in the catalyst. The differential heat of propene adsorption in this range (78 ± 2 kJ mol^{-1}) is quite high, which indicates strong adsorption of propene on energetically homogeneous adsorption sites. Further increase in surface coverage leads to a gradual decrease in the heat of adsorption up to a coverage of 29 μmol g^{-1} that corresponds to 2.9% of total molybdenum atoms in the catalyst where another plateau is approached. The heat of adsorption (22 kJ mol^{-1}) is close to the value measured on SBA-15 (Figure 3B). Notably, the concentration of strong adsorption sites (16 μmol g^{-1} within the first plateau) coincides with the active site density estimated by active site counting after the catalysis (15 μmol g^{-1}, Table 1). The consistency strongly suggests the relevance of sites titrated by propene adsorption in the microcalorimetric experiment to the genesis of active carbene species.

Strong interaction of propene with MoO_x/SBA-15 is also reflected in the Langmuir constant. The Langmuir adsorption equation has been formally applied to model the measured adsorption isotherms (lines in Figure 3C) neglecting that chemical transformations are probably involved in adsorption of propene on MoO_x/SBA-15 using eq 2,[35]

$$N_{ads} = N_{mono}\frac{Kp}{1 + Kp} \quad (2)$$

where N_{ads} is the amount of propene adsorbed at equilibrium pressure p, N_{mono} is the monolayer adsorption capacity, and K is the Langmuir constant, which is the ratio of the rate constant of adsorption and desorption describing the strength of adsorption. The fit curve for the MoO_x/SBA-15 depicted in Figure 3C deviates from the data points above ∼20 μmol g^{-1}, which indicates that the propene uptake in this high coverage region is predominantly due to a different type of adsorption mechanism. The part of the adsorption isotherm curve of the catalyst above 20 μmol g^{-1} is roughly parallel to the curve of SBA-15 (Figure 3C), suggesting that the same type of physisorption on silica species and/or inert molybdenum oxide species becomes predominant at the higher coverage. This view is also supported by the faster decay of the heat evolution upon adsorption (vide infra, Figure 4). A Langmuir fit taking into account data of propene adsorption on MoO_x/SBA-15 up to a coverage of ∼16 μmol g^{-1}, where a quasi-constant and high heat of adsorption was found, yielded K = 8.6

dx.doi.org/10.1021/ja3011989 | J. Am. Chem. Soc. 2012, 134, 11462−11473

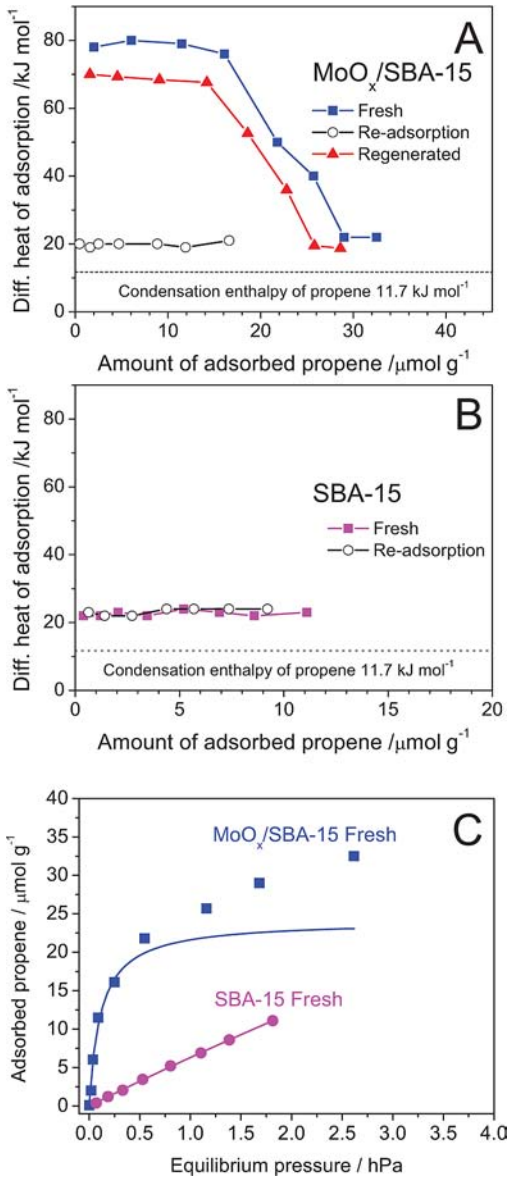

Figure 3. Propene adsorption studied by microcalorimetry at 323 K on MoO_x/SBA-15 and SBA-15 pretreated in O_2 at 823 K and at 20 kPa for 0.5 h; differential heat as a function of the amount of adsorbed propene on MoO_x/SBA-15 (A) and SBA-15 (B); readsorption profiles were measured after evacuation at $\sim 10^{-3}$ Pa for 2 h; the regeneration was performed applying the same procedure as the initial pretreatment (in O_2 at 823 K and at 20 kPa for 0.5 h); the adsorption isotherm of propene over MoO_x/SBA-15 and SBA-15 measured at 323 K is shown in (C); measured data points up to an amount of adsorbed propene of 16 μmol g^{-1} were used to fit the data of MoO_x/SBA-15 based on the Langmuir equation.

$\pm$ 2.8 hPa^{-1}, whereas the fit for propene adsorption on SBA-15 including the entire data points resulted in a much lower value of K = 0.039 $\pm$ 0.001 hPa^{-1}. These results clearly indicate strong adsorption of propene on a small fraction of molybdenum oxide surface sites on MoO_x/SBA-15.

Propene adsorption on SBA-15 is fully reversible. In contrast, the readsorption profile measured on MoO_x/SBA-15 after evacuation (Figure 3A) was almost identical to the adsorption profile measured on bare SBA-15 (Figure 3B), which evidences again strong and irreversible adsorption of propene on MoO_x sites during the first adsorption cycle. In accordance with this

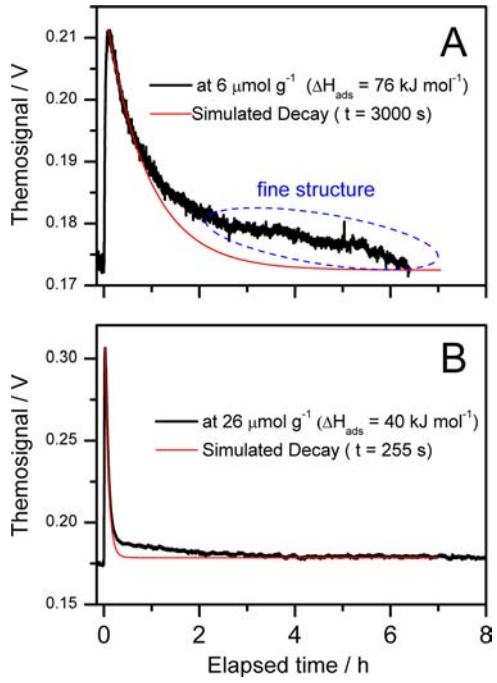

Figure 4. Evolution of the heat signals upon propene adsorption at 323 K on MoO_x/SBA-15 (pretreated in 20% O_2 at 823 K for 0.5 h) at the cumulative adsorption amount of 6 (A) and 26 μmol g^{-1} (B).

observation, the integral heat of desorption measured during the evacuation after the first adsorption steps was much lower than the integral heat of adsorption. Apparently, irreversible surface reactions happen, which contribute substantially to the heat signal measured during the first propene adsorption experiment. These reactions are most likely related to the formation of the active sites.

Evaluation of the kinetics of the heat evolution allows further insight into the adsorption process. The response of the exothermic signals in the range of the first plateau of propene adsorption on MoO_x/SBA-15 (at coverage of 6 μmol g^{-1}) shows an extremely slow decay continuing for $\sim$7 h (Figure 4A). In contrast, the evolution of heat at higher coverage (Figure 4B), where the differential heat of adsorption is slightly higher than the heat of propene adsorption measured on SBA-15 (at a coverage of 26 μmol g^{-1}), is relatively quickly completed. The initial decay of the heat signals was evaluated applying an exponential decay model as described in eq 3,

$$I(t) = I_0 \exp(-t/\tau) \quad (3)$$

wherein $I(t)$ is the net thermosignal intensity at time t, I_0 is the maximum of the net thermosignal intensity after an increment of dosing pressure, t is the elapsed time after reaching the I_0, and τ is the time constant. The calculated time constants are about 3000 and 255 s for 6 and 26 μmol g^{-1}, respectively (Figure 4). The latter value approximately matches the time constant of the calorimeter used, indicating weak and reversible adsorption. The significantly increased time constant at low coverage indicates that the adsorption is superimposed by slow surface reactions. The deviation of the fit curve at prolonged times (Figure 4A) is due to the occurrence of secondary exothermic processes that are supposed to be consecutive reactions of adsorbed species. The deviation is less pronounced for the adsorption at 26 μmol g^{-1} reflecting the predominance of reversible adsorption in accordance with the moderate

dx.doi.org/10.1021/ja3011989 | J. Am. Chem. Soc. 2012, 134, 11462–11473

differential heat of adsorption (40 kJ mol^{-1}). These observations indicate that the strong and irreversible adsorption involves slow and probably consecutive reactions on the surface, which might be related to the genesis of the molybdenum carbene sites. The sustaining generation of heat for ~7 h bears resemblance to the slow evolution of metathesis activity over 10−15 h, which are required to reach steady state activity (Figure 2).

3.4. IR Study of Propene and Subsequent Ethene-d_4 Adsorption. Microcalorimetry revealed irreversible and possibly reactive adsorption of propene on MoO_x/SBA-15 up to a certain level of coverage. The chemical reactions are presumably associated with the genesis of the active carbene sites. We employed in situ IR spectroscopy at the same temperature (323 K) to obtain information about the nature of the surface species involved in the processes occurring upon propene adsorption on the MoO_x/SBA-15 surface. The equilibrium pressure of propene was adjusted initially to p = 3 hPa, which corresponds to complete coverage of strong adsorption sites according to the results of microcalorimetry. A reference experiment using SBA-15 showed no adsorbed species that persist after evacuation, which is consistent with the reversible adsorption found by microcalorimetry.

3.4.1. Progressive Formation of Isopropoxide and Acetone upon Propene Adsorption. After propene dosing for 0.5 h and subsequent evacuation, the spectrum (magenta line in Figure 5A) features bands due to the stretching modes of C−H bonds in methyl groups at 2983, 2939, and 2880 cm^{-1}, and the corresponding deformation modes at 1465, 1455, 1390, and 1377 cm^{-1}. Notably, characteristic C−H stretching bands of olefinic methylene species[36,37] at ~3010 and at ~3090 cm^{-1} as well as C═C stretching mode at 1610−1650 cm^{-1} are not detected, indicating the absence of C═C bonds in strongly adsorbed species that persist evacuation at 323 K. Thus, strong adsorption involves a reaction, which leads to conversion of the olefinic C═C bond in propene. The detected peak patterns agree well with the bands of isopropoxy species adsorbed on the surface of metal oxides.[38−41] In fact, adsorption of isopropanol on MoO_x/SBA-15 results in a quite similar spectrum (Figure S4 (1) of the SI), confirming that isopropoxide is the major species formed by adsorption of propene at 323 K on MoO_x/SBA-15. The transformation of propene into isopropoxide happens via protonation of the olefin by acidic surface OH groups. Accordingly, the detection of surface isopropoxy species confirms the presence of Brønsted acid sites on the surface of MoO_x/SBA-15 in agreement with ammonia adsorption (Figure 1B) and clearly indicates involvement of Brønsted acidity in the surface reactions of adsorbed propene.

After the 18 h of propene dosing and subsequent evacuation, (blue line in Figure 5A), all of the bands became considerably more intense, which evidence progressive slow adsorption as found by microcalorimetry. Moreover, new bands at 1668 and 1417 cm^{-1} are clearly visible, which can be assigned to the C═O stretching mode of the carbonyl group and the deformation mode of methyl groups, respectively, of coordinated acetone.[38,40,42,43] Occurrence of these bands upon acetone adsorption (Figure S4 (3) of the SI) as well as the development of a similar carbonyl stretching band at 1673 cm^{-1} upon prolonged (18 h) isopropanol adsorption (Figure S4 (2) of the SI) corroborate the formation of acetone by oxidation of isopropoxide surface species. The modest intensity of the carbonyl band at 1668 cm^{-1} (blue line in Figure 5A) compared

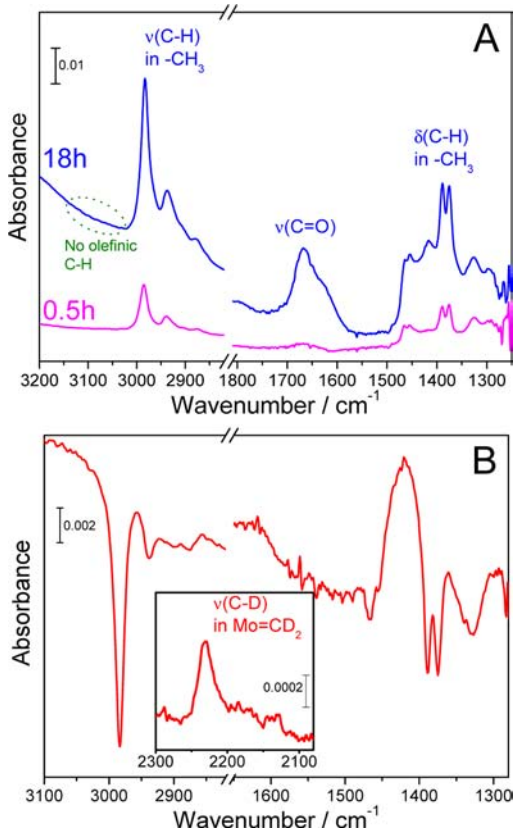

Figure 5. IR spectra recorded after propene adsorption on MoO_x/SBA-15 for 0.5(magenta) and 18 h (blue) and subsequent evacuation (A). The difference spectrum shown in (B) was obtained by subsequent ethene-d_4 dosing at p = 3 hPa and T = 323 K for 18 h and evacuation using the blue spectrum in (A) as subtrahend. Propene was dosed at 323 K and 3.0 hPa after the pretreatment in 20 kPa of O_2 at 823 K for 0.5 h. The inset in (B) shows the frequency range of the C−D stretching.

to the spectrum of acetone adsorption (Figure S4 (3) of the SI) suggests that only a fraction of the isopropoxide species undergo oxidation into acetone. Formation of acetone implies the involvement of surface molybdenum oxide species acting as oxidizing agent and resulting in partial reduction of molybdenum on the silica surface. Essentially the same observation has been reported for alumina-supported molybdena catalysts. The formation of isopropoxide and the consecutive oxidation to acetone upon propene adsorption takes place on MoO_x/Al_2O_3 even at room temperature.[40,41] Besides the formation of acetone, the broad peaks arising in the range 1550−1650 cm^{-1} and below 1490 cm^{-1} (Figure 5A) imply the gradual accumulation of various other surface deposits, such as carboxylates[44] or enolates.[45]

3.4.2. Validation of Metathesis Activity of the Resulting Surface. The metathesis activity of the resulting surface was confirmed by testing the reactivity with ethene-d_4. After propene adsorption for 18 h and subsequent evacuation, an equilibrium pressure of p = 3 hPa ethene-d_4 was adjusted at 323 K in the IR cell. Under these conditions, surface Mo−alkylidene species, if present, should be transformed into deuterium-labeled Mo−methylidene species (eq 1). The spectrum presented in Figure 5B was obtained after dosing ethene-d_4 followed by evacuation using the spectrum before the ethene-d_4 dosing (blue line in Figure 5A) as background. The negative peaks due to C−H stretching modes at 2984, 2939, 2898, and

dx.doi.org/10.1021/ja3011989 | J. Am. Chem. Soc. 2012, 134, 11462−11473

Scheme 3. Proposed Route for the Carbene Formation Starting from a Mo(VI) Site upon Interaction with Two Propene Molecules[a]

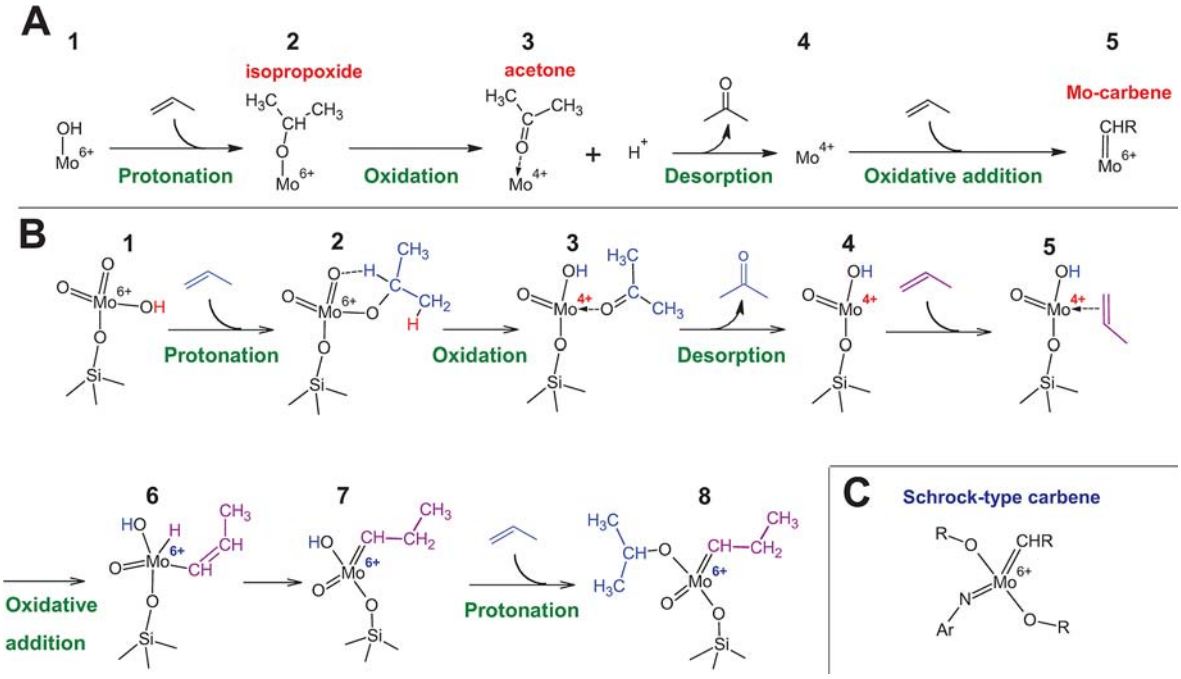

[a]General scheme (A), a scheme assuming a tetrahedral dioxo structure as the pre-catalyst (B) compared to the structure of reference Schrock-type homogeneous catalysts (C).[63]

2877 cm^{-1} and C−H deformation modes at 1468, 1389, and 1375 cm^{-1}, and the appearance of C−D stretching modes at 2100−2300 cm^{-1} (Figure 5B inset) evidence the exchange of stable (not removable by evacuation) surface organic species into ethene-d_4 originated surface species most likely due to a metathesis reaction catalyzed by surface Mo−carbene sites. The negative peaks due to C−H stretching modes agree well with the bands of Mo−ethylidene species at 2985, 2910, 2890, and 2850 cm^{-1},[46] indicating the presence of this species before dosing of ethene-d_4. The positions of the observed C−D stretching modes at 2230 and 2160−2200 cm^{-1} are close to those reported for deuterated methylidene ($Mo{=}CD_2$) species detected on MoO_x/SiO_2 (2245 and 2160 cm^{-1}),[47] which further corroborates the presence of Mo−carbene sites on the surface of MoO_x/SBA-15 and the metathesis activity of the catalyst surface, which has been generated during the IR experiment of propene adsorption. The intensities of the negative peaks due to C−H stretching modes (Figure 5B) are low compared to the original spectrum (blue line in Figure 5A), indicating that the concentration of carbene species is low in contrast to the concentration of other surface species, e.g., the remaining isopropoxide species.

3.4.3. Summary of the Propene Adsorption IR Study. The IR study revealed that adsorbed propene is slowly protonated on the catalyst surface to yield isopropoxide, which undergoes oxidation to give acetone. These reactions require bifunctionality of the catalyst in terms of concurrent abundance of Brønsted acid sites and redox active molybdena centers. The evolution of Mo−carbene species evidenced by ethene-d_4 adsorption indicates that these processes are related to the genesis of the active Mo−carbene sites. We relate the very slow generation of isopropoxide and acetone as observed by IR spectroscopy to the prolonged heat generation registered in the microcalorimetric experiment (Figure 3A) and to the retarded evolution of the metathesis activity (Figure 2).

4. DISCUSSION

4.1. Quantity and Quality of Active Carbene Sites. Investigation of MoO_x/SBA-15 by the postreaction active site titration detected the expected metathesis product (i.e., $CD_2{=}CH{-}CH_3$) formed by reaction of surface Mo−ethylidene species with the probe ethene-d_4 ($CD_2{=}CD_2$) (Table 1), providing evidence that the Chauvin mechanism (Scheme 2) is operative over supported molybdena catalysts.

The titration experiment reveals that only 1.5% of the molybdenum atoms in the catalyst belong to the pool of active carbene centers. Accordingly, it is extremely challenging to establish structure−activity relationships, because structural characterization generally displays an average picture of the variety of species usually present on the catalyst surface. A strategy that allows selective detection of the essential information is certainly necessary to distinguish catalytically relevant surface sites from spectator species. The present approach takes these considerations into account and tackles the task by applying a combination of microcalorimetry and IR spectroscopy for investigation of propene adsorption on the catalyst surface at the reaction temperature.

Quantification of active sites by titrative metathesis allows the determination of an average intrinsic metathesis activity per active site, i.e., the measurement of turnover frequencies in the strict sense of molecular catalysis. This is a rare case in heterogeneous catalysis due to frequently encountered difficulties in quantification of active sites, which often lead to the wrong assumption that all atoms of a specific catalyst component contribute to the activity. Accordingly, the data in the literature, which allow a reliable comparison of turnover frequencies for MoO_x/SBA-15 catalysts, are rather limited.

dx.doi.org/10.1021/ja3011989 | J. Am. Chem. Soc. 2012, 134, 11462−11473

Instead, homogeneous catalysts anchored on silica may represent suitable reference systems. The optimized Schrock-type Mo−alkylidene complexes, which are among the most active propene metathesis catalysts, show, when anchored on silica, much higher turnover frequencies (e.g., TOF of 1.9 s^{-1} at 303 K) than MoO_x/SBA-15 (~0.15 s^{-1}, Table 1).[48] The difference probably arises from a different geometric and electronic structure of the carbene centers. Substantial influence of the structure on the activity has been demonstrated for structurally well-defined catalysts prepared by grafting of organometallic complexes on silica.[49] The structure sensitivity has been confirmed by theoretical studies, in which various anchoring configurations of oxo-molybdenum carbene sites on silica[50] and alumina were considered.[51−55]

MoO_x/SBA-15 contains molybdenum atoms in a multitude of different geometric arrangements, which are hardly distinguishable by spectroscopic techniques. Therefore, we follow a bottom-up approach starting with the elucidation of the building mechanism of the active carbene sites, which comprise only the minor fraction of Mo atoms that are characterized by a specific and catalytically favorable local geometric environment.

4.2. Formation Route of Carbene Sites. The genesis of Mo−carbene sites is a consequence of the reaction between surface molybdena species and the reactant propene.

The pseudo-Wittig mechanism (Scheme 1D) has persisted to be the only mechanism for three decades since Rappe and Goddard proposed it based on purely theoretical considerations. However, the detected high heat of propene adsorption (78 ± 2 kJ mol^{-1}, Figure 3A) is not in accord with this route. The pseudo-Wittig mechanism has estimated significantly positive Gibbs energies for the carbene formation, especially in the case of supported molybdena catalysts[56−58] (e.g., ΔG_{300} = +16 kJ mol^{-1} for the reaction of Cl_2MoO_2 and ethene; estimated by an ab initio calculation,[21] ΔE = ca. +60 kJ mol^{-1} for the reaction of a supported molybdena (Mo(VI)-oxo centers in a β zeolite cluster with propene; estimated by a DFT calculation[57]). Accordingly, the pseudo-Wittig mechanism is a thermodynamically unfavorable route. In previous experimental reports concerning fully oxidized supported W[24] and Re[7] catalysts, the detection of carbonyl compounds during the genesis of metathesis activity and the dependency of the reactivity from the type of reacting olefin have been considered as experimental proofs for the pseudo-Wittig mechanism.[7,24] On the basis of our calorimetric and spectroscopic findings during the genesis of metathesis activity, we propose an alternative mechanism (Scheme 3), which is not in contradiction with the reported experimental results mentioned above.

On the surface of MoO_x/SBA-15, molybdenum occurs in its highest oxidation state in form of highly dispersed surface molybdenum oxide species that comprise terminating oxo (Mo═O) groups. Brønsted acidity, probably originated by Mo−OH groups, and Lewis acidity due to coordinatively unsaturated Mo(VI) centers are found to be present as well (Section 3.1).

The quantitative agreement between the concentrations of strong adsorption sites found by microcalorimetry (Figure 3A) and the postreaction active site titration (Table 1) suggests that the strong exothermic adsorption of propene on the catalyst is in relationship with the genesis of the carbene sites.

IR spectroscopy provides the explanation for the exothermic events during the propene adsorption. The IR spectra for propene and subsequent ethene-d_4 adsorption revealed the slow formation of isopropoxy species followed by oxidation to coordinated acetone (Figure 5A) during the genesis of metathesis activity (Figure 5B). Experimental[59] and theoretical[59−61] studies have shown that formation of surface isopropoxide readily occurs by protonation upon adsorption of an olefin on Brønsted acidic catalysts with the heat of olefin adsorption of about 80−100 kJ mol^{-1}. These values agree well with the differential heats of propene adsorption measured by microcalorimetry (Figure 3). Having evidence for the presence of Brønsted acid sites in the catalyst (Figure 1B, Figure 5A), we consider that the major event upon propene adsorption is the formation of isopropoxide species through protonation of the olefin by Brønsted acid sites.

The subsequent event detected by IR spectroscopy during the genesis of the metathesis activity is the formation of coordinated acetone (Figure 5A). Although the formation of carbonyl compounds is in line with the pseudo-Wittig mechanism (Scheme 1D), it is rather reasonable to consider that carbonyl compounds are formed through oxidation of the isopropoxy intermediate on the redox-active MoO_x/SBA-15 catalyst. It is well-known that the oxidation of propene to acetone via the isopropoxy intermediate takes place with acidic molybdena based mixed oxide catalysts at relatively low (393−473 K) temperature.[62] We consider that the same type of reaction occurs in the present case. The formation of a carbonyl compound should involve the reduction of molybdenum centers, i.e., Mo(VI) to Mo(IV), if the reduction takes place at a single molybdenum atom.

Importantly, coordinatively unsaturated monomeric Mo(IV) centers are known to be good precursors of Mo−carbene sites that are formed via an oxidative addition of the propene molecule to Mo(IV) surface species.[15,16,64−66] Actually, most of highly active molybdenum oxide-based metathesis catalysts are prepared via efficient creation of coordinatively unsaturated monomeric Mo(IV) centers by a reductive pretreatment of the catalyst.[46,64] This inspires us to propose a new route for the carbene formation presented in Scheme 3A.

The first step involves the reduction of Mo(VI) to Mo(IV) via formation of an isopropoxy species by an acid−base reaction and the subsequent oxidative dehydrogenation of the isopropoxide intermediate to acetone (Scheme 3A, 1−3). The second step includes desorption of acetone followed by an oxidative addition of another propene molecule to the Mo(IV) center to form the active Mo(VI)-carbene species (Scheme 3A, 3−5). Consequently, bifunctionality of the catalyst comprehending Brønsted acidity and the ability to accomplish oxidative dehydrogenation is considered as an essential requirement for the first step. The carbene formation via an oxidative addition of a propene molecule to Mo(IV) is a well established event,[15,16,64−66] which likely takes place via 1,2-hydrogen shift mechanism (as shown in Scheme 1A). The positive effect of acidity in olefin metathesis is well recognized by the observation that the use of acidic silica−alumina supports yields relatively active catalysts.[67−69] It is also known that reducibility is relevant to the metathesis activity.[70] The present proposal is quite consistent with these facts and provides a mechanistic explanation for the role of acidity and reducibility. The slow development of the metathesis activity (Figure 2) compared to silica−alumina supported molybdena catalysts[10−12] might be related to the limited acidity of MoO_x/SBA-15. Considering progressive slow formation of isopropoxide and acetone in the in situ IR experiment, these surface

dx.doi.org/10.1021/ja3011989 | J. Am. Chem. Soc. 2012, 134, 11462−11473

reactions (Scheme 3A 1−3) most likely represent the kinetic bottleneck of the evolution of active carbene sites. It is noted that the color of the catalyst bed remained white during the metathesis reaction, suggesting the absence of reduced molybdenum centers. Probably, the desorption of acetone and subsequent oxidative addition of propene (Scheme 3A 3−5) are much faster than the foregoing steps in the case of MoO_x/SBA-15, which gives rise to a very small concentration of the Mo(IV) intermediate.

Besides Brønsted acidity and reducibility, the formation of Mo−carbene species requires desorption of the coordinated acetone (Scheme 3A, 3−4) and subsequent oxidative addition of another propene molecule (Scheme 3A, 4−5). We consider that strict dehydration of the catalyst and abundant presence of propene molecules are indispensable requirements to achieve these steps. The oxidation of the olefin to a carbonyl compound via the alkoxy intermediate (Scheme 3A, 1−4) is accelerated by the presence of water;[62] whereas, water as well as carbonyl compounds are known to inhibit the metathesis reaction.[63,71,72] Although the presence of water might be favorable for the oxidation of propene via an alkoxy intermediate (Scheme 3A, 1−4), it is expected that the presence of water or carbonyl compounds lead to the decomposition of carbene sites, or more likely, disturb the carbene formation (Scheme 3A, 4−5) by blocking Mo(IV) sites. In fact, we observed lower catalytic activity accompanied by the color change of the catalyst from white to bluish when we use a less purified propene feed (i.e., the reaction was done using the same propene feed but without placing the water-trapping silica guard beds above and below the catalyst bed (see the SI for experimental details)), while the catalyst color remained white after 15 h of time on stream in standard reaction condition. The blue coloration observed in the experiment using less purified feed indicates the formation of reduced molybdenum species that are stabilized and blocked by the adsorption of water ligands, which suggests that the oxidative addition of propene was disturbed, likely by water contamination. It is well-known that pretreatment of the catalyst at elevated temperature (typically 773−873 K) in dry atmosphere is certainly necessary to obtain the catalytic activity. We consider that the dehydrated surface acts as an efficient trap for acetone and any byproduct of the reaction between surface molybdena with propene allowing the access of the second propene molecule to Mo(IV) sites, which leads to the generation of carbene species. It has been established that surface molybdena[73] and silanol groups[33] undergo structural reconstruction during the dehydration at elevated temperature, leaving surface sites which readily absorb water[33] and acetone.[74] Probably, the presence of this kind of dehydrated sites on the catalyst in a dry propene feed facilitates efficient trapping of acetone and access of the second propene molecule, allowing the formation of carbene sites (Scheme 3A, 3−5). In fact, we detected no carbonyl compounds (e.g., acetone) in the reactor effluent during the propene metathesis by mass spectrometry, indicating that generated carbonyl compounds are trapped on the catalyst surface.

To prove these assumptions, we have performed an additional experiment, which validated the hypothesis established here and succeeded in improving the catalytic performance. Before starting the metathesis reaction, we inserted a propene adsorption−desorption pretreatment. After the standard oxidative regeneration, the MoO_x/SBA-15 catalyst was exposed to neat propene at 300 K followed by thermal treatment in flowing argon at 823 K applying a temperature program with a heating rate of 10 K min^{-1}. As a consequence, we succeeded to double the activity and to eliminate the induction period (Figure 6). The heating after propene

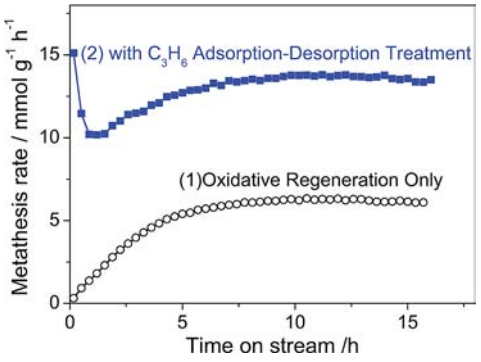

Figure 6. Propene metathesis activity of MoO_x/SBA-15 (323 K, contact time = 0.35 s g mL^{-1}) after different regeneration procedures. (1) Standard oxidative regeneration (20% O_2 flow at 823 K for 0.5 h) was performed. (2) In addition to the standard oxidative regeneration, the catalyst was treated in neat propene flow at 300 K for 1 h followed by heat treatment in argon flow at 823 K (heating rate 10 K min^{-1}) for 0.5 h.

adsorption at 300 K accelerates the oxidation of surface isopropoxide species, forming Mo(IV) sites. During further temperature rise, desorption of oxidation products (oxygenates and possibly water) is accelerated, which leaves bare Mo(IV) sites that are the precursors of the active carbene sites in metathesis. Thus, the heating has two effects: promotion of oxidation and desorption of the oxidation products. We demonstrate here how a knowledge-based approach efficiently improves catalytic performance. Systematic optimization of the activation protocol as well as the control of catalyst structure according to the present knowledge is required to improve the catalytic performance further.

We further consider the suggested route and criteria of carbene formation is applicable to other important heterogeneous metathesis catalysts, i.e., supported tungsten(VI) oxide and rhenium(VII) oxide. These oxides are also acidic, reducible, and deposited on "desiccant-like" high surface area supports. The reducibility decreases in the order Re(VII) > Mo(VI) > W(VI) in general; this ranking is in agreement with the activity in olefin metathesis. These facts are quite consistent with the present conclusion.

4.3. Molecular Structure of the Carbene Sites. According to the proposed mechanism, successful precatalyst sites should fulfill multiple functions, namely, Brønsted acidity, capability to perform isopropoxide oxidation and trapping capacity with respect to acetone and water. Apparently, only few grafted molybdenum oxide species simultaneously meet all of these criteria. It is, therefore, understandable why only 1.5% of the existing molybdenum atoms take place in catalysis.

Raman (Figure S1 of the SI) and UV−vis (Figure S2 of the SI) spectroscopy suggest that monomeric dioxo molybdena species in tetrahedral geometry are the predominant species,[28,31,75−77] although a certain amount of non-nomomeric molybdena species probably coexist.[12,78,79] Monomeric molybdena has been suggested to be the relevant catalyst precursors.[12] In homogeneous metathesis, four-coordinated monomeric Mo(VI)−alkylidene species represent the common general structure of active Mo-based metathesis catalysts.[63] In accordance with this fact, recent DFT calculations[52,55,80] as well

dx.doi.org/10.1021/ja3011989 | J. Am. Chem. Soc. 2012, 134, 11462−11473

as experimental studies[16,47] using well-defined catalysts with low Mo loadings have confirmed the metathesis activity of four-coordinated monomeric Mo(VI)−alkylidene species in the class of supported Mo catalysts. Furthermore, if the oxidation of isopropoxide occurs at nonmonomeric molybdena having Mo−O−Mo bonding, the two-electron reduction of molybdenum (i.e., oxidation of isopropoxide to acetone) may possibly result in the formation of two Mo(V) centers instead of the formation of a Mo(IV) site that is the precursor of a carbene site. Monomeric molybdena species are likely surrounded by reactive silanol groups and Si−O−Si bonds created during the high-temperature pretreatment step, which provide the trapping function. Hence, monomeric molybdena species and resulting monomeric Mo(VI)−alkylidene species are the most likely candidates for precatalysts and active sites. Taking into account the presence of Mo−OH groups (i.e., Brønsted acid sites) and their involvement in the formation of carbene species, we propose geometrically accessible tetrahedral monomeric dioxo species with a molybdenol group (Scheme 3B 1) as a candidate for the relevant precatalyst.

Scheme 3B describes the detailed scheme assuming the 1,2-hydrogen shift mechanism (Scheme 1A) in the oxidative addition step (Scheme 3B 5−7). Upon the formation of acetone (Scheme 3B 2−3), the released proton is likely hosted by the oxo oxygen on the same molybdenum atom in cooperation with concurrent reduction of the molybdenum atom, leaving a new molybdenol group (Scheme 3B 3). It is speculated that this molybdenol further undergoes addition of another propene molecule to yield an isopropoxide group owing to its acidic character (Scheme 3B, 7−8). Accordingly, the final molecular structure of Mo carbene species (Scheme 3B, 8) features an isopropoxide group, an anchoring Mo−O−Si bond, an oxo group, and an alkylidene group. Actually, this structure is an analogue of Schrock-type Mo(VI)−alkylidene complexes (Scheme 3C).[63] While Schrock-type complexes comprise two alkoxy ligands and an imido ligand besides the alkylidene ligand, the suggested surface Mo(VI)−alkylidene has an oxo ligand and an anchoring bond instead of an imido ligand and an alkoxy ligand, respectively. Insight obtained in the present study allows us to clearly envisage the molecular structure of active sites in supported transition metal oxide-derived heterogeneous catalysts, opening a possibility to address the material gap between homogeneous and heterogeneous catalysts. Further information concerning the molecular structure of the precursor surface molybdenum oxide species that can readily undergo transformation to Mo−carbene sites will bring deeper understanding and will allow the rational design of the catalyst. The specifically low turnover frequency of the present system indicates that the actual carbene structure is not optimal and improvements might be possible. Modification of the electronic structure of the active centers by appropriate support modification is the design target mimicking the N-containing ligands of the molecular analogues.

5. CONCLUSIONS

We contribute to understanding in catalysis through structural identification of active sites on the surface of a heterogeneous, meso-structured molybdenum oxide model catalyst for propene metatheses applying operando techniques on a strictly quantitative level. The genesis of active sites in such a system is a demanding in situ and one-pot synthesis of metal carbene species from surface metal oxides, which involves Brønsted acid−base chemistry, oxidation−reduction processes, byproduct capture, and oxidative addition. In the present propene metathesis over MoO_x/SBA-15, only 1.5% of total Mo atoms accomplish this process. The mechanistic insight into the genesis of active carbene sites obtained by microcalorimetry and in situ IR delivers the explanation for the low abundance of active species, and provides the criteria for successful molecular structures of the precatalyst, which allows us to envisage resulting configurations of metal carbenes by applying established general mechanisms of acid−base and red-ox chemistry. To our surprise, we find structural similarity between the anticipated surface Mo(VI)−alkylidene and highly active Schrock-type catalysts. This encourages us to implement inputs from homogeneous catalysis in prospective catalyst synthesis approaches.

We embark two strategies toward catalyst improvement based on the gained insight: (1) controlling the surface carbene synthesis, and (2) knowledge-based design of the precatalyst.

Concerning strategy (1), the simple temperature pretreatment (Figure 6) demonstrates that favorable activation conditions can assist the carbene formation disclosing a great and, in particular, easy option. Moreover, further control and optimization of the alkyl ligand in the carbene species should be possible by extending the choice of activating reagents instead of using merely the reactant itself. For example, use of isobutene instead of propene would facilitate the formation of the alkoxide intermediate due to increased stability of the *tert*-butoxide. In addition, the presence of the bulky *tert*-butoxide group at the final carbene site would contribute to improve the stability of the carbene species. Another option would be the use of alcohols (e.g., methanol, *tert*-butanol) for efficient creation of reduced metal centers (i.e., precursor for the carbene sites). By using alcohols, Brønsted acid sites are not necessarily required. The knowledge in homogeneous catalysis and organometallic synthesis will strongly contribute to the selection of prospective activating agents.

Strategy (2) benefits from the spatial separation of metal species that can be accomplished on the surface of a heterogeneous catalyst. Irreversible anchoring prevents self-condensation of complexes, which is a major difficulty in homogeneous catalysis. The presence of highly reactive molybdenol groups accounting for Brønsted acidity can be implemented within transition metal oxide species anchored on solid surfaces. Synthesis of isolated surface molybdenum oxide moieties having molybdenol ligands is a specific target, since our microcalorimetry results indicate that the amount of Brønsted acid sites is a limiting factor with respect to the number of active centers in the final catalyst.

Building bridges in catalysis research on the basis of our case study propene metathesis, we demonstrate here that the highly interdisciplinary field of heterogeneous catalysis will find more solid link to related fields in chemistry through in-depth understanding.

■ ASSOCIATED CONTENT

Supporting Information

Nitrogen adsorption data, Raman and UV−vis spectra of the calcined catalyst and support, IR spectra of isopropanol and acetone adsorption, as well as experimental details. This material is available free of charge via the Internet at http://pubs.acs.org.

dx.doi.org/10.1021/ja3011989 | J. Am. Chem. Soc. 2012, 134, 11462−11473

AUTHOR INFORMATION

Corresponding Author

trunschke@fhi-berlin.mpg.de

Notes

The authors declare no competing financial interest.

ACKNOWLEDGMENTS

The authors thank M. Hashagen for her help with the IR experiments, G. Lorenz for measuring N_2 physisorption, Dr. F. Girgsdies, and E. Kitzelmann for performing XRD analysis, Dr. T. Cotter for Raman experiments, and A. Klein-Hoffmann for XRF measurements. Dr. B. Frank is acknowledged for valuable discussion. This work was conducted in the framework of the COE "UniCat" (www.unicat.tu-berlin.de) of the German Science Foundation. K.A. is grateful to Mitsubishi Gas Chemical Co. Inc. for a fellowship.

REFERENCES

(1) Dumesic, J. A.; Huber, G. W.; Boudart, M. In *Handbook of Heterogeneous Catalysis*, 2nd ed.; Wiley-VCH: Weinheim, 2008; pp 1−15.
(2) Somorjai, G. A.; Li, Y. *Introduction to Surface Chemistry and Catalysis*; 2nd ed.; John Wiley & Sons: Hoboken, NJ, 2010.
(3) Libuda, J.; Freund, H.-J. *Surf. Sci. Rep.* **2005**, *57*, 157−298.
(4) Rupprechter, G.; Weilach, C. *J. Phys.: Condens. Matter* **2008**, *20*, 184019.
(5) Handzlik, J.; Ogonowski, J. *Catal. Lett.* **2003**, *88*, 119−122.
(6) Chauvin, Y. *Angew. Chem., Int. Ed.* **2006**, *45*, 3740−3747.
(7) Salameh, A.; Copéret, C.; Basset, J.-M.; Böhm, V. P. W.; Röper, M. *Adv. Synth. Catal.* **2007**, *349*, 238−242.
(8) Chauvin, Y.; Commereuc, D. *J. Chem. Soc., Chem. Commun.* **1992**, 462−464.
(9) Mol, J. *J. Mol. Catal. A: Chem.* **2004**, *213*, 39−45.
(10) Debecker, D. P.; Stoyanova, M.; Colbeau-Justin, F.; Rodemerck, U.; Boissière, C.; Gaigneaux, E. M.; Sanchez, C. *Angew. Chem., Int. Ed.* **2012**, *51*, 2129−2131.
(11) Debecker, D. P.; Bouchmella, K.; Stoyanova, M.; Rodemerck, U.; Gaigneaux, E. M.; Mutin, P. H. *Catal. Sci. Technol.* **2012**, *2*, 1157−1164.
(12) Debecker, D. P.; Schimmoeller, B.; Stoyanova, M.; Poleunis, C.; Bertrand, P.; Rodemerck, U.; Gaigneaux, E. M. *J. Catal.* **2011**, *277*, 154−163.
(13) Debecker, D. P.; Stoyanova, M.; Rodemerck, U.; Gaigneaux, E. M. *J. Mol. Catal. A: Chem.* **2011**, *340*, 65−76.
(14) Debecker, D.; Bouchmella, K.; Poleunis, C.; Eloy, P.; Bertrand, P.; Gaigneaux, E.; Mutin, P. *Chem. Mater.* **2009**, *21*, 2817−2824.
(15) Iwasawa, Y.; Hamamura, H. *J. Chem. Soc., Chem. Commun.* **1983**, 130−132.
(16) Iwasawa, Y.; Kubo, H.; Hamamura, H. *J. Mol. Catal.* **1985**, *28*, 191−208.
(17) McCoy, J. R.; Farona, M. F. *J. Mol. Catal.* **1991**, *66*, 51−58.
(18) Farona, M. F.; Tucker, R. L. *J. Mol. Catal.* **1980**, *8*, 85−90.
(19) Grubbs, R. H.; Swetnick, S. J. *J. Mol. Catal.* **1980**, *8*, 25−36.
(20) Laverty, D. T.; Rooney, J. J.; Stewart, A. *J. Catal.* **1976**, *45*, 110−113.
(21) Rappe, A. K.; Goddard, W. A. *J. Am. Chem. Soc.* **1982**, *104*, 448−456.
(22) Grünert, W.; Stakheev, A. Y.; Feldhaus, R.; Anders, K.; Shpiro, E. S.; Minachev, K. M. *J. Catal.* **1992**, *135*, 287−299.
(23) Chen, X.; Zhang, X.; Chen, P. *Angew. Chem., Int. Ed.* **2003**, *42*, 3798−3801.
(24) Basrur, A. G.; Patwardhan, S. R.; Was, S. N. *J. Catal.* **1991**, *127*, 86−95.
(25) Howman, E. J.; Mgcrath, B. P.; Williams, K. V. *Catalyst regeneration process*. British Patent 1,144,085, March 5, 1969.
(26) Zhao, D.; Feng, J.; Huo, Q.; Melosh, N.; Fredrickson, G. H.; Chmelka, B. F.; Stucky, G. D. *Science* **1998**, *279*, 548−552.
(27) Thielemann, J. P.; Weinberg, G.; Hess, C. *ChemCatChem* **2011**, *3*, 1814−1821.
(28) Tian, H.; Roberts, C. A.; Wachs, I. E. *J. Phys. Chem. C* **2010**, *114*, 14110−14120.
(29) Hu, H.; Wachs, I. E.; Bare, S. R. *J. Phys. Chem.* **1995**, *99*, 10897−10910.
(30) Vuurman, M. A.; Wachs, I. E. *J. Mol. Catal.* **1992**, *77*, 29−39.
(31) Lee, E. L.; Wachs, I. E. *J. Phys. Chem. C* **2007**, *111*, 14410−14425.
(32) Dieterle, M.; Weinberg, G.; Mestl, G. *Phys. Chem. Chem. Phys.* **2002**, *4*, 812−821.
(33) Davydov, A. *Molecular Spectroscopy of Oxide Catalyst Surface*; John Wiley & Sons Ltd.: Chichester, 2003.
(34) Zhang, B.; Li, Y.; Lin, Q.; Jin, D. *J. Mol. Catal.* **1988**, *46*, 229−241.
(35) Langmuir, I. *J. Am. Chem. Soc.* **1916**, *38*, 2221−2295.
(36) Grabowski, R.; Efremov, A.; Davydov, A.; Haber, E. *Kinet. Catal.* **1981**, *22*, 794−797.
(37) Efremov, A.; Lokhov, Y.; Davydov, A. *Kinet. Catal.* **1981**, *22*, 969−975.
(38) Martín, C.; Rives, V.; Sánchez-Escribano, V.; Busca, G.; Lorenzelli, V.; Ramis, G. *Surf. Sci.* **1991**, *251−252*, 825−830.
(39) Finocchio, E.; Busca, G.; Lorenzelli, V.; Willey, R. J. *J. Chem. Soc., Faraday Trans.* **1994**, *90*, 3347.
(40) Goncharova, O.; Davydov, A. *React. Kinet. Catal. Lett.* **1983**, *23*, 285−289.
(41) Davydov, A.; Efremov, A. *Kinet. Catal.* **1983**, *24*, 1214−1220.
(42) Efremov, A.; Davydov, A. *React. Kinet. Catal. Lett.* **1981**, *18*, 363−366.
(43) Goncharova, O.; Davydov, A.; Yureva, T. *Kinet. Catal.* **1984**, *25*, 124−129.
(44) Sanchez Escribano, V.; Busca, G.; Lorenzelli, V. *J. Chem. Phys.* **1991**, *95*, 5541−5545.
(45) Efremov, A. A.; Davydov, A. A. *React. Kinet. Catal. Lett.* **1981**, *18*, 353−356.
(46) Vikulov, K. A.; Shelimov, B. N.; Kazansky, V. B. *J. Mol. Catal.* **1991**, *65*, 393−402.
(47) Vikulov, K. A.; Elev, I. V.; Shelimov, B. N.; Kazansky, V. B. *J. Mol. Catal.* **1989**, *55*, 126−145.
(48) Blanc, F.; Rendon, N.; Berthoud, R.; Basset, J.-M.; Coperet, C.; Tonzetich, Z. J.; Schrock, R. R. *Dalton Trans.* **2008**, 3156−3158.
(49) Rendón, N.; Berthoud, R.; Blanc, F.; Gajan, D.; Maishal, T.; Basset, J.-M.; Copéret, C.; Lesage, A.; Emsley, L.; Marinescu, S. C.; Singh, R.; Schrock, R. R. *Chem.—Eur. J.* **2009**, *15*, 5083−5089.
(50) Handzlik, J. *J. Phys. Chem. B* **2005**, *109*, 20794−20804.
(51) Handzlik, J. *J. Catal.* **2003**, *220*, 23−34.
(52) Handzlik, J. *Surf. Sci.* **2007**, *601*, 2054−2065.
(53) Handzlik, J.; Ogonowski, J.; Tokarz-Sobieraj, R. *Catal. Today* **2005**, *101*, 163−173.
(54) Handzlik, J. *Surf. Sci.* **2004**, *562*, 101−112.
(55) Handzlik, J.; Sautet, P. *J. Catal.* **2008**, *256*, 1−14.
(56) Li, X.; Guan, J.; Zheng, A.; Zhou, D.; Han, X.; Zhang, W.; Bao, X. *J. Mol. Catal. A: Chem.* **2010**, *330*, 99−106.
(57) Guan, J.; Yang, G.; Zhou, D.; Zhang, W.; Liu, X.; Han, X.; Bao, X. *Catal. Commun.* **2008**, *9*, 2213−2216.
(58) Li, X.; Zheng, A.; Guan, J.; Han, X.; Zhang, W.; Bao, X. *Catal. Lett.* **2010**, *138*, 116−123.
(59) Campbell, K. A.; Janik, M. J.; Davis, R. J.; Neurock, M. *Langmuir* **2005**, *21*, 4738−4745.
(60) Kazansky, V. B. *Catal. Today* **1999**, *51*, 419−434.
(61) Engelhardt, J.; Hall, W. K. *J. Catal.* **1995**, *151*, 1−9.
(62) Moro-oka, Y. *Appl. Catal., A* **1999**, *181*, 323−329.
(63) Schrock, R. R.; Hoveyda, A. H. *Angew. Chem., Int. Ed.* **2003**, *42*, 4592−4633.
(64) Iwasawa, Y.; Ichinose, H.; Ogasawara, S.; Soma, M. *J. Chem. Soc., Faraday Trans. 1* **1981**, *77*, 1763−1777.

(65) Shelimov, B. N.; Elev, I. V.; Kazansky, V. B. *J. Mol. Catal.* **1988**, *46*, 187−200.
(66) Elev, I.; Shelimov, B.; Kazansky, V. *Kinet. Catal.* **1989**, *30*, 787−792.
(67) Handzlik, J.; Ogonowski, J.; Stoch, J.; Mikolajczyk, M.; Michorczyk, P. *Appl. Catal., A* **2006**, *312*, 213−219.
(68) Aritani, H.; Fukuda, O.; Yamamoto, T.; Tanaka, T.; Imamura, S. *Chem. Lett.* **2000**, 66−67.
(69) Debecker, D. P.; Hauwaert, D.; Stoyanova, M.; Barkschat, A.; Rodemerck, U.; Gaigneaux, E. M. *Appl. Catal., A* **2011**, *391*, 78−85.
(70) Thomas, R.; Moulijn, J. A. *J. Mol. Catal.* **1982**, *15*, 157−172.
(71) Mol, J. C.; Leeuwen, P. W. N. M. *Metathesis of Alkens in "Handbook of Heterogeneous Catalysis*, 2nd ed.; Wiley-VCH: Weinheim, 2008.
(72) Dinger, M. B.; Mol, J. C. *Organometallics* **2003**, *22*, 1089−1095.
(73) Boer, M.; Dillen, A. J.; Koningsberger, D. C.; Geus, J. W.; Vuurman, M. A.; Wachs, I. E. *Catal. Lett.* **1991**, *11*, 227−239.
(74) Crocellà, V.; Cerrato, G.; Magnacca, G.; Morterra, C. *J. Phys. Chem. C* **2009**, *113*, 16517−16529.
(75) Lee, E. L.; Wachs, I. E. *J. Phys. Chem. C* **2008**, *112*, 6487−6498.
(76) Chempath, S.; Zhang, Y.; Bell, A. T. *J. Catal.* **2007**, *111*, 1291−1298.
(77) Guo, C. S.; Hermann, K.; Hävecker, M.; Thielemann, J. P.; Kube, P.; Gregoriades, L. J.; Trunschke, A.; Sauer, J.; Schlögl, R. *J. Phys. Chem. C* **2011**, *115*, 15449−15458.
(78) Thielemann, J. P.; Kröhnert, J.; Hess, C. J. *Phys. Chem. C* **2010**, *114*, 17092−17098.
(79) Thielemann, J. P.; Ressler, T.; Walter, A.; Tzolova-Müller, G.; Hess, C. *Appl. Catal., A* **2011**, *399*, 28−34.
(80) Handzlik, J. *J. Phys. Chem. C* **2007**, *111*, 9337−9348.